LAWRENCE
LIVERMORE
NATIONAL
LABORATORY

UCRL-CONF-220496

# Simulating Effects of Non-Isothermal Flow on Reactive Transport of Radionuclides Originating from an Underground Nuclear Test

S F Carle, M Zavarin, D E Shumaker, A F B Tompson, R M Maxwell, G A Pawloski

April 10, 2006

Computational Methods in Water Resources XVI
Copenhagen, Denmark
June 19, 2006 through June 22, 2006

UCRL-CONF-220496

# SIMULATING EFFECTS OF NON-ISOTHERMAL FLOW ON REACTIVE TRANSPORT OF RADIONUCLIDES ORIGINATING FROM AN UNDERGROUND NUCLEAR TEST

STEVEN F. CARLE[1], MAVRIK ZAVARIN[1], DAN SHUMAKER[1], ANDREW TOMPSON[1], REED MAXWELL[1], AND GAYLE PAWLOSKI[1]

[1]Lawrence Livermore National Laboratory, L-208, POB 808, Livermore, CA 94551

## ABSTRACT

Temperature can significantly affect radionuclide transport behavior. In simulation of radionuclide transport originating from an underground nuclear test, temperature effects from residual test heat include non-isothermal groundwater flow behavior (e.g. convection cells), increased dissolution rates of melt glass containing refractory radionuclides, changes in water chemistry, and, in turn, changes in radionuclide sorption behavior. The low-yield (0.75 kiloton) Cambric underground nuclear test situated in alluvium below the water table offers unique perspectives on radionuclide transport in groundwater. The Cambric test was followed by extensive post-test characterization of the radionuclide source term and a 16-year pumping-induced radionuclide migration experiment that captured more mobile radionuclides in groundwater. Discharge of pumped groundwater caused inadvertent recirculation of radionuclides through a 220-m thick vadose zone to the water table and below, including partial re-capture in the pumping well. Non-isothermal flow simulations indicate test-related heat persists at Cambric for about 10 years and induces limited thermal convection of groundwater. The test heat has relatively little impact on mobilizing radionuclides compared to subsequent pumping effects. However, our reactive transport models indicate test-related heat can raise melt glass dissolution rates up to $10^4$ faster than at ambient temperatures depending on pH and species activities. Non-isothermal flow simulations indicate that these elevated glass dissolution rates largely decrease within 1 year. Thermally-induced increases in fluid velocity may also significantly increase rates of melt glass dissolution by changing the fluid chemistry in contact with the dissolving glass.

## 1. BACKGROUND

1.1. **Nevada Test Site and UGTA Project**. The U.S. Department of Energy conducted 839 underground nuclear tests between 1951 and 1992 [U.S. Department of Energy, 2000]. Of these 839 tests, 828 were conducted at the Nevada Test Site (NTS) in southern Nevada (Figure 1). Some underground nuclear tests at NTS, particularly those detonated below the water table, have released radionuclides into groundwater. The U.S. Department of Energy sponsors environmental restoration activities including an “Underground Test Area” (UGTA) project to define hydrologic boundaries encompassing groundwater resources that may be unsafe for domestic or municipal use.

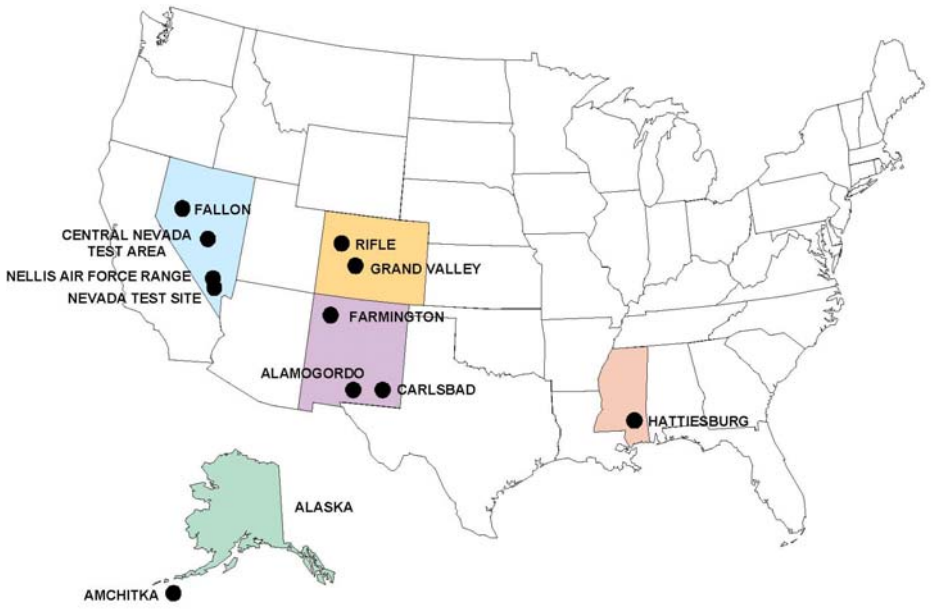


FIGURE 1. United States Nuclear Test Locations – Nevada Test Site and other [U.S. Department of Energy, 2000].

1.2. **Test Phenomenology.** Detonation of a nuclear device instantly vaporizes the test canister and releases an immense amount of energy producing high temperatures and pressures and shock waves. In the underground setting, water is vaporized and surrounding rock is vaporized, melted, and compressed in radial succession away the test location (Figure 2) [Germain and Kahn, 1968; Borg et al.,1976; Office of Technology Assessment, 1989]. The spherical vaporized zone or "cavity" reaches maximum size within tenths of a second after detonation. Within seconds, as gas pressures dissipate and temperatures cool, gas components begin to condense in order of their relative vapor pressure, first of which are the rock and refractory radionuclides (e.g., actinides). Molten rock lining the cavity walls accumulates as a puddle at the bottom of the cavity. Test-induced pressure and compression may induce mounding of the water table.

Within minutes to hours, the overlying rock collapses into the cavity to form a "chimney" of collapse debris that may extend to the ground surface. Collapse rubble partially mixes with the melt puddle to form a "melt glass zone." Groundwater will begin to refill the cavity if the detonation point was initially below the water table. Formation of the chimney opens void space and, thus, initializes lower pressure and under-saturated conditions in the chimney [Knox et al., 1965; Borg et al., 1976; Burkhard and Rambo, 1991]. The final configuration of test-induced alteration includes a melt glass zone in the lower portion of the former cavity, a cylindrical "chimney" of collapse debris above the melt glass zone, and a spherical shell of compressed and crushed rock immediately adjacent to the former cavity except where collapsed above.

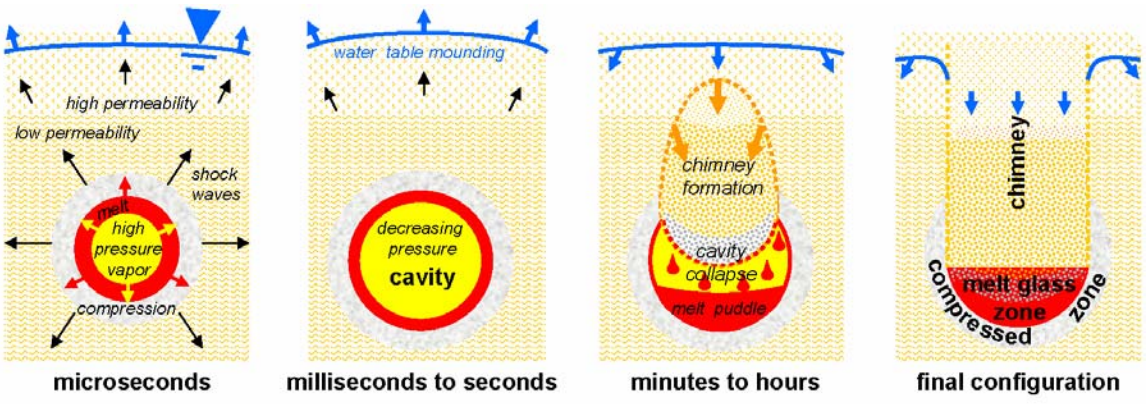


FIGURE 2. Generalized early-time phenomenology resulting detonation of an underground nuclear test in alluvium below the water table.

1.3. **The Cambric Test.** The Cambric underground nuclear test, a low-yield test of 0.75 kilotons equivalent TNT, was detonated in 1965 in alluvium 294 m below ground surface and 74 m below the water table at Frenchman Flat, NTS (Figure 3). Cavity radius is estimated at 12.9 to 13.7 m based on test yield [Pawloski, 1999] and subsequent post-test drill-back characterization. Within days after the Cambric test, mixing of collapse debris and boiling of groundwater cooled the melt glass zone to an estimated 170 $^{o}$C, which is slightly below the boiling point for water at hydrostatic pressure of 74 m below the water table. Once boiling has ceased, cooling within the test cavity continues by thermal conduction and convection by groundwater flow. Meanwhile, groundwater flow through high permeability alluvium above the detonation point enabled the water table to recover and the chimney to re-saturate. Thermal and pressure effects induced by underground nuclear tests can affect the subsurface for many years [Burkhard and Rambo, 1991; Carle et al.. 2003; Halford et al., 2005].

1.4. **The Cambric Radionuclide Migration Experiment.** The Cambric test offers rare insights into radionuclide migration because a unique field experiment was conducted beginning ten years after detonation. In 1974, nine years after the Cambric test, a slanted borehole RNM-1 was drilled and sampled for radionuclides through the upper chimney, former cavity, melt glass zone and below. These sample data were used to characterize the radionuclide "source term" attributed to the Cambric test. From 1975 through 1991, groundwater was pumped steadily at rates between 1,650 and 3,280 m$^3$/day from well RNM-2S located 91 m to the south and screened 24 to 47 m below the center of the Cambric nuclear test cavity (Figure 3). The purpose of this vigorous long-term pumping was to capture tritium released from the Cambric test into groundwater, monitor for any other radionuclides, and provide data on migration of radionuclides under an induced hydraulic gradient [Hoffman et al., 1977; Bryant, 1992]. Pumping effluent was discharged into a nearby unlined ditch and regularly monitored for test-related radionuclide content, which eventually included more mobile species such as tritium ($^3$H), $^{14}$C, $^{36}$Cl, $^{85}$Kr, $^{129}$I, and, possibly, $^{237}$Np [Bryant, 1992; Finnegan and Thompson, 2002]. Relatively immobile species known to occur at other detonation sites, such as $^{90}$Sr, $^{137}$Cs, and $^{238,239}$Pu, were not detected.

Between 1991 and 1993, regular groundwater monitoring indicated rising levels of tritium at well UE-5n, located over 500 m from the Cambric emplacement hole (U-5e) and screened near the water table about 106 m northeast of the Cambric drainage ditch (Figure 3). However, well UE-5n is distant from transport pathways between the Cambric test cavity and well RNM-2S. Because well UE-5n is located relatively close to the drainage ditch, these measurements suggest

groundwater pumped from RNM-2S, including radionuclides originating from the Cambric test, leaked from the drainage ditch and reached the water table [Tompson et al., 2006]. Mechanisms for radionuclide transport and recirculation through a 220 m thick vadose zone are examined in further detail by Maxwell et al. [2006].

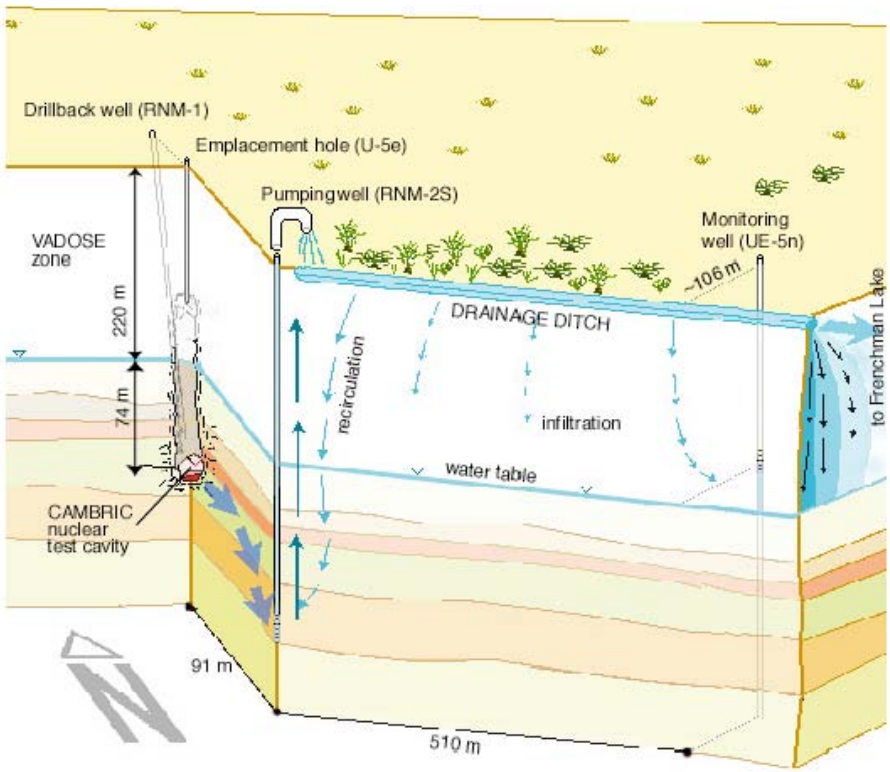


FIGURE 3. Schematic of the Cambric radionuclide migration experiment in Frenchman Flat, Nevada Test Site, Nevada [Tompson et al., 2006].

.

## 2. NON-ISOTHERMAL FLOW SIMULATION

As part of the UGTA project, we are focusing on numerical simulation of non-isothermal groundwater flow and radionuclide transport associated with the Cambric test. The focus of this paper is on how to integrate the impact of test-related heat into simulation of radionuclide transport processes. Transient flow including pumping and ditch discharge, variable saturation, and coupled heat and groundwater flow (including variable groundwater density and viscosity) are simulated using the finite-difference code NUFT [Nitao, 1999]. Resolution in the flow

simulations ranges from two meters near the test-altered zones and 5 meters or less toward the pumping well RNM-2S, with telescopic increase out to distant boundaries. Non-linear reactive transport processes are simulated using a transient streamline-based approach [Pawloski et al., 2001] described in Section 3, with streamline paths defined from the transient and non-isothermal flow fields simulated by NUFT.

2.1. **Flow Simulation and Calibration**. The hydrogeologic conceptual model assumes a stacked sequence of alluvial layers (Figure 4, left), which were characterized in detail at well ER-5-4 [Warren et al., 2002] and correlated to previous characterization work at well UE-5n [Ramspott and McArthur, 1977]. We calibrated layer permeabilities to data from a multiple-well aquifer test with pumping at well RNM-2S and drawdown response at RNM-1, RNM-2, RNM-2S, and ER-5-4. The permeability field was also calibrated to tritium breakthrough measured at well RNM-2S from the 1975-1991 Cambric radionuclide migration experiment (Figure 4, right).

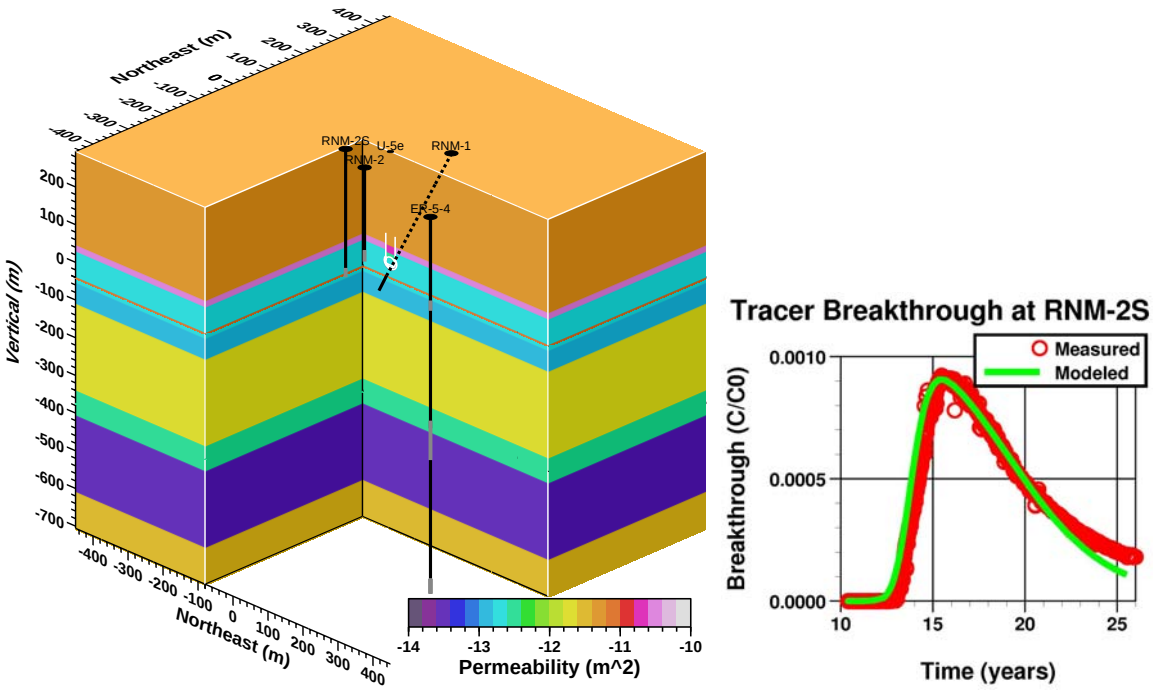


FIGURE 4. Permeability field used for flow and transport simulation (left) calibrated by flow modeling to tracer (test-related tritium) breakthrough at the pumping well RNM-2S (right). Nearby wells and boreholes are shown in black with screened intervals in gray. Test altered zones are outlined in white.

NUFT was used to simulate transient temperature, saturation, tracer concentration, and hydraulic head (as deduced from pressure and fluid density fields) fields (Figure 5). In Figure 5, location of the drainage ditch is assumed parallel to the negative portion of the "Northwest" axis. The ambient groundwater flow direction is assumed parallel to the "Northeast" axis. The simulated temperature field at 10.4 years after the Cambric test, just prior to pumping at RNM-2S, shows a few degrees $^{o}$C of residual test heat superposed on a geothermal gradient. At 12.3 years, the simulated saturation field shows the effects of infiltration along the drainage ditch. At 15.9 years, the simulated tracer concentration field, with source origin corresponding to test-related tritium, reaches a peak at the pumping well RNM-2S (Figure 4, right) and is migrating

through the vadose zone and beginning to reach the water table. Simulated hydraulic head at 25.5 years after the test, near the end of the Cambric radionuclide migration experiment in 1991, shows the cone of depression at RNM-2S and water table mounding beneath infiltration from the drainage ditch.

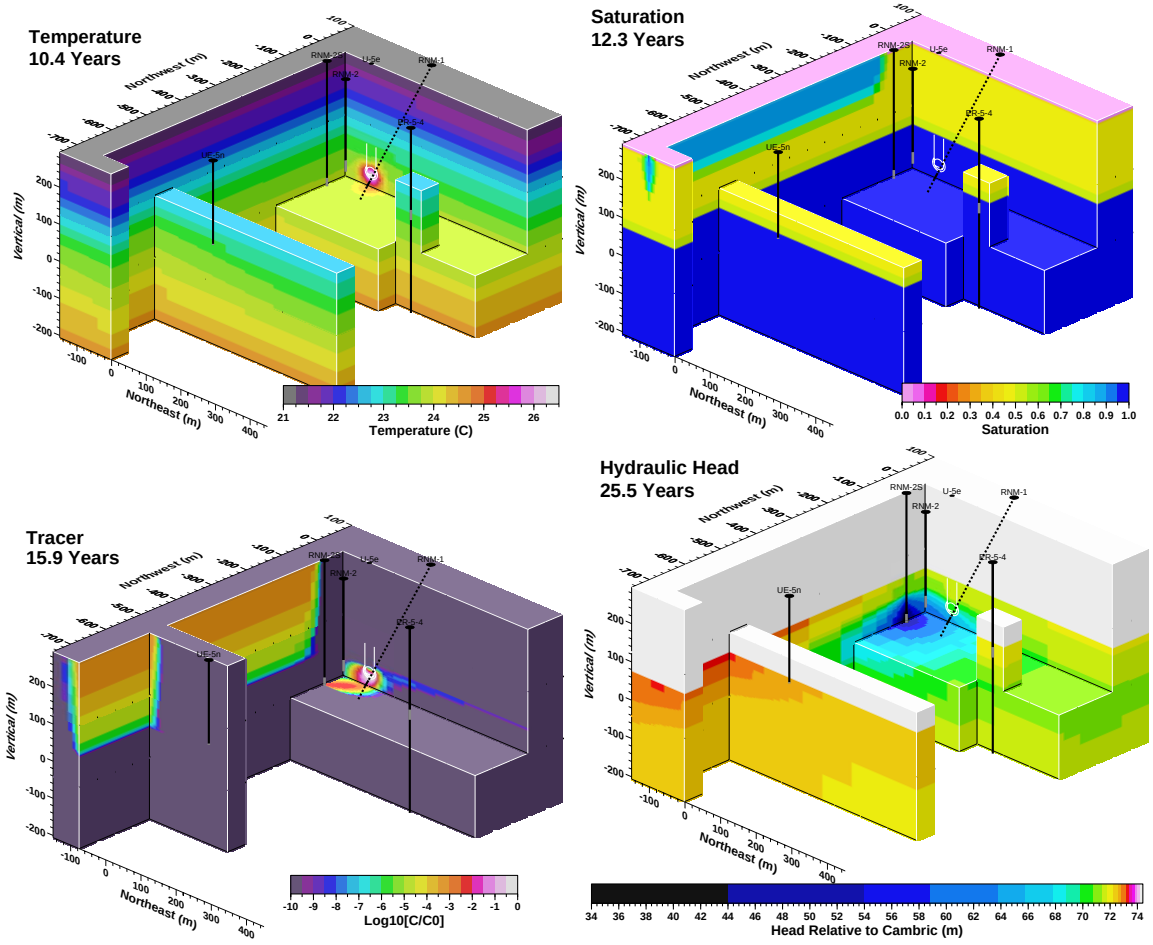


FIGURE 5. Three-dimensional large-scale cutaway views of NUFT simulations of temperature field at 10.4 years (upper left), saturation field at 12.3 years (upper right), tracer (test-related tritiated water) at 15.9 years (lower left), and hydraulic head at 25.5 years (lower right) after the Cambric test. Test altered zones outlined in white.

2.2. **Consideration of Test-Related Heat**. The calibrated local three-dimensional flow field described above is resolved to 2 m grid blocks within test-altered zones including the cavity, melt glass zone, compressed zone, and lower chimney. Flow simulation initial conditions assign an initial temperature of 170 $^{o}$C in the melt glass zone and 40 $^{o}$C in the former cavity (Figure 6) based on early-time phenomenology including boiling processes [Carle et al., 2003]. Within ten years after the test (before pumping at RNM-2S), the simulated temperature field decays in the test-altered zones primarily by thermal diffusion to a maximum test-related temperature anomaly of about 2-3 $^{o}$C.

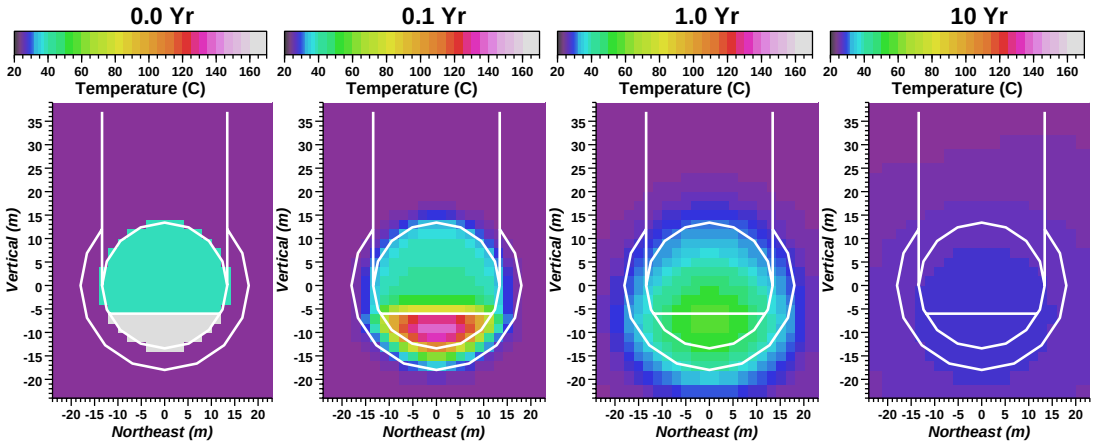


FIGURE 6. Cross sectional views of NUFT simulation of temperature fields in the test-altered zones at 0.0, 0.1, 1.0, and 10 years.

As melt glass zone temperature decays (Figure 7, left), the NUFT flow simulations include consideration of the variation of fluid density and viscosity with temperature and pressure. Flow velocity fields subsequent to the Cambric test are affected by test-related heat, pumping at well RNM-2S, and the ambient groundwater flow. Substantial increases in melt glass zone fluid velocity occur within one year of the test (Figure 7, right). Decrease in fluid density by thermal expansion from test-related residual heat can induce convection cells with significant upward component to groundwater flow [Pawloski et al., 2001]. According to the NUFT simulation, thermal effects on the groundwater flow velocity field in the Cambric melt glass zone were maximized between about 0.03 to 0.10 years after the test. Pumping induced effects on melt glass fluid velocity are evident between 10 and 26 years after the test.

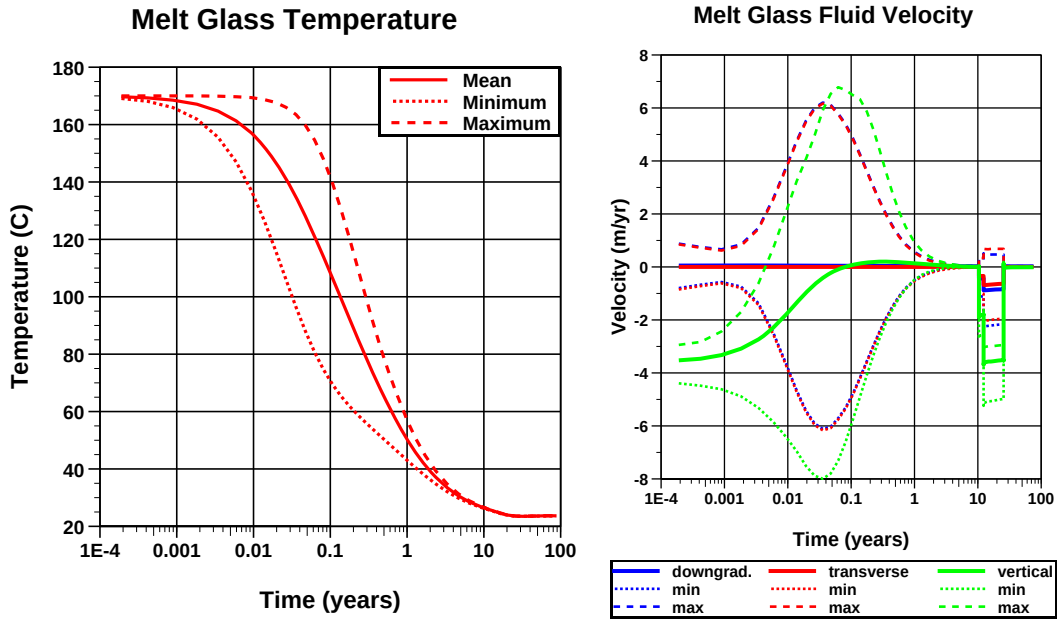


FIGURE 7. NUFT simulation of mean, minimum, and maximum melt glass zone temperature (left), and mean (solid lines), minimum (dotted lines), and maximum (dashed lines) fluid velocities in downgradient, transverse, and vertical directions (right).

The NUFT flow simulation indicates test heat would induce a flow circulation pattern in the melt glass zone with downward flow directions on the outside and upward flow near the center (Figure 8, left) and flow velocity magnitudes 2 to 3 times greater than ambient thermal conditions (Figure 8, right). However, the thermal flow field transients are relatively short lived compared to RNM-2S pumping-induced changes in flow velocity (Figure 8, center). By 50 years after the test, long after test-related heat and pumping effects have dissipated, the flow field returns to ambient conditions (Figure 8, right).

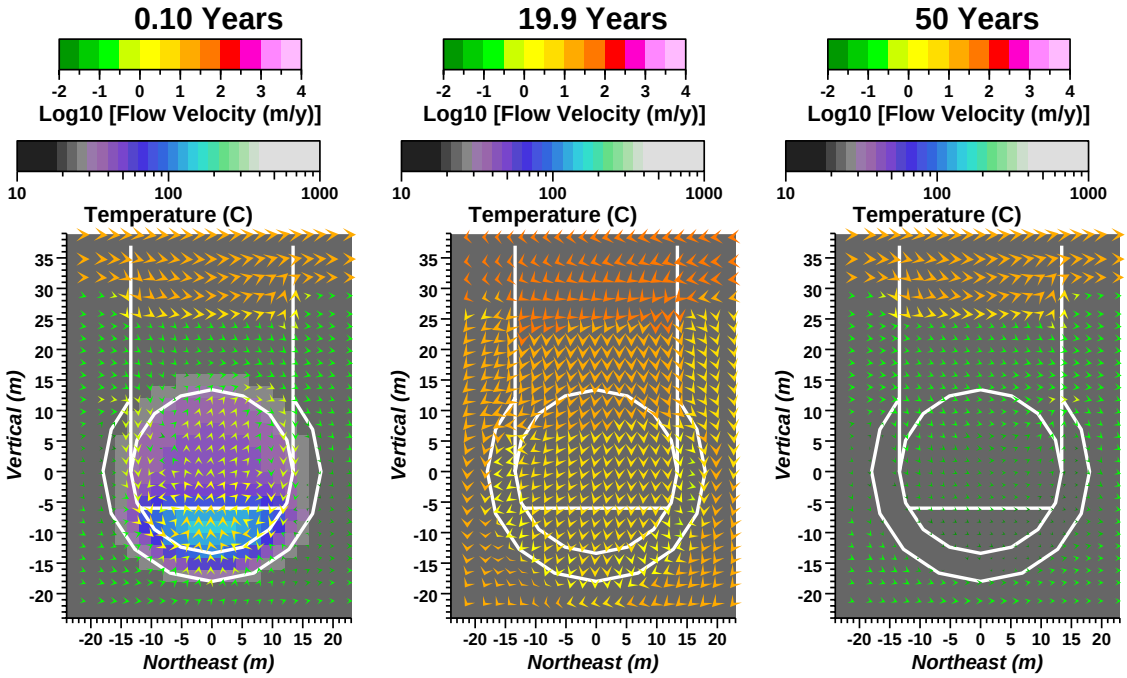


FIGURE 8. NUFT simulation of groundwater flow velocity vector fields near test-altered zones showing impacts of test related heat (left), pumping from nearby well RNM-2S (center), and ambient groundwater flow (right). Arrows point in flow velocity direction with color and size indicating magnitude of velocity. Background color shows temperature.

## 3. REACTIVE TRANSPORT SIMULATION

3.1. **Streamline Method and Reactive Transport Model.** We employ a "streamline" method in conjunction with a multi-component reactive transport model to simulate three-dimensional reactive transport of radionuclides originating from the Cambric test. The streamline method is designed to reduce computational burden in two ways: (1) by focusing calculations on the regions where concentrations of chemical species of interest are significant and (2) by approximating three-dimensional reactive transport processes as a collection of one-dimensional reactive transport processes occurring along transient flow paths or "streamlines." Compared to the total of 308,637 grid cells in the flow simulation, the maximum number of points of computation traced by streamlines reaches only about 20,000.

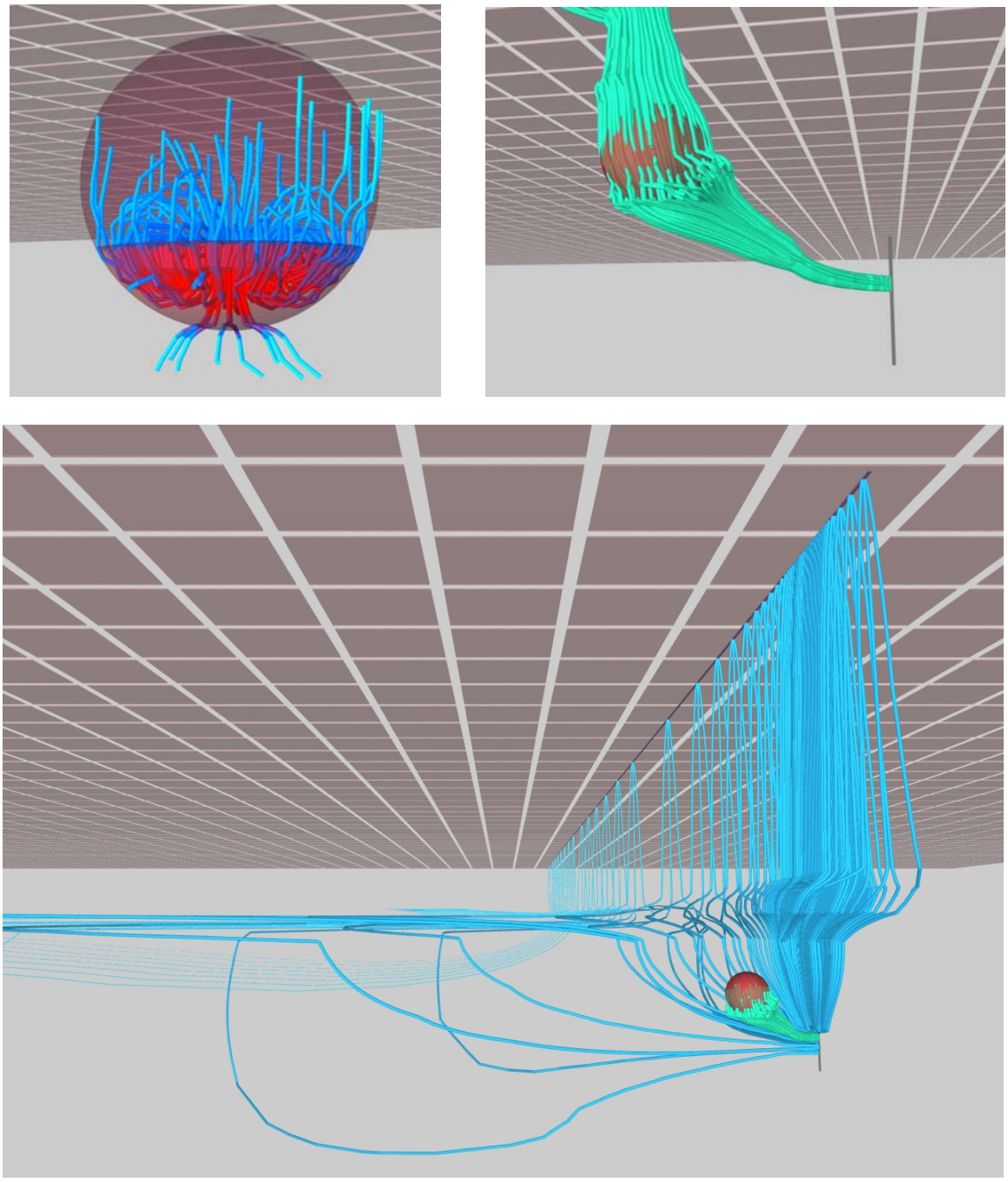

FIGURE 9. Streamline traces originating from melt glass zone at 0.1 years (upper left) and subsequently evolved through the pumping stage between 10.4 and 25.6 years for locations between Cambric source and pumping well (upper right) and overall flow system (below).

Flow velocities, porosities, and saturations from the NUFT non-isothermal flow simulations are used to prescribe streamline traces (Figure 9) and fluxes. Pollock [1988] provides the fundamental computational method to determine streamlines given the three-dimensional flow field. The integration of the product of time-of-flight across grid cells and streamline flux determines the volumetric discretization along which the 1-D reactive transport processes are

simulated. The flux also determines the contribution from each streamline to the total three-dimensional transport.

Streamlines for the Cambric simulations originate from the spherical shaped source volume where radionuclides are assumed to be initially deposited by the test, which includes the melt glass zone, cavity, compressed zone, and lower chimney. Under transient flow and transport conditions, the streamline paths evolve with time. The results of each streamline time segment are collected and integrated into three-dimensional grids of concentrations. Streamline paths are re-initialized according to updated concentration and flow velocity fields.

The one-dimensional reactive transport processes are simulated on streamlines using the CRUNCH code, an updated version of the Global Implicit Multi-component Reactive Transport (GIMRT) code developed by Steefel and Yabusaki [1996]. CRUNCH simulates multi-component mass transport in porous media under non-isothermal conditions, including consideration of zonal variations in mineralogy and fluid chemistry. Aqueous speciation, surface complexation, ion exchange, mineral dissolution/precipitation, and radionuclide decay are all modeled explicitly. CRUNCH implicitly couples advection, diffusion, and chemical reaction processes occurring over each time step. The temperature along each streamline is imported from the NUFT non-isothermal flow simulation.

3.2. **Consideration of Thermal Effects.** Temperature affects radionuclide transport primarily by accelerating groundwater flow velocities, melt glass dissolution rates, and secondary mineral precipitation rates. Most long-lived radionuclides associated with an underground nuclear test are initially incorporated into melt glass. Silicate melt glass dissolution rate is strongly temperature-dependent and provides a radiologic source term to groundwater. Glass dissolution and secondary mineral precipitation reactions may also alter the near-field water chemistry which will, in turn, alter the aqueous speciation, surface complexation, and ion exchange processes that retard radionuclide transport and affect glass dissolution rates.

Secondary mineral precipitation depends on a range of conditions including the composition of the silicate glass, the temperature, pH, and groundwater composition. In general, zeolites form over a temperature range of 100 to 250ºC. At lower temperatures, a variety of clays are more likely to form. At higher temperatures, feldspars and other aluminosilicates are likely to form. Geochemical modeling suggests that when clay precipitation dominates, the pH tends to rise. This rise in pH affects both the sorption behavior of radionuclides and the overall rate of glass dissolution, as described below.

We simulate temperature-dependent rate of glass dissolution, *r(T)*, in (mol-glass $m^{-2}$ $sec^{-1}$) using the transition state theory (TST) model

$$r(T) = k_0 \times e^{\frac{E_a}{R}\left(\frac{T-T_0}{T_0 T}\right)} \times \prod_i a_i^{n_i} \times \left(1 - \left(\frac{Q}{K(T)}\right)^{1/\sigma}\right)^{\upsilon} \qquad (1)$$

where $k_0$ is the far-from-saturation glass dissolution rate (mol-glass $m^{-2}$ $sec^{-1}$) at temperature $T_0$, $E_a$ is the activation energy (cal $mol^{-1}$) accounting for change in glass dissolution as a function of temperature, $R$ is the gas constant (1.99 cal $mol^{-1}$ $K^{-1}$), $T$ and $T_0$ are the temperature of interest and the reference temperature (typically 25°C), respectively, $a_i^n$ are a series of dissolution inhibiting or promoting solution aqueous species activities to power $n$, $Q$ is the saturation of the solution relative to the temperature-dependent solubility product of the glass ($K(T)$). The terms $\sigma$ and $\upsilon$ are empirical terms often included in the dissolution/precipitation model. Similar equations are used to define dissolution and precipitation rates of secondary minerals that form as a result of glass dissolution.

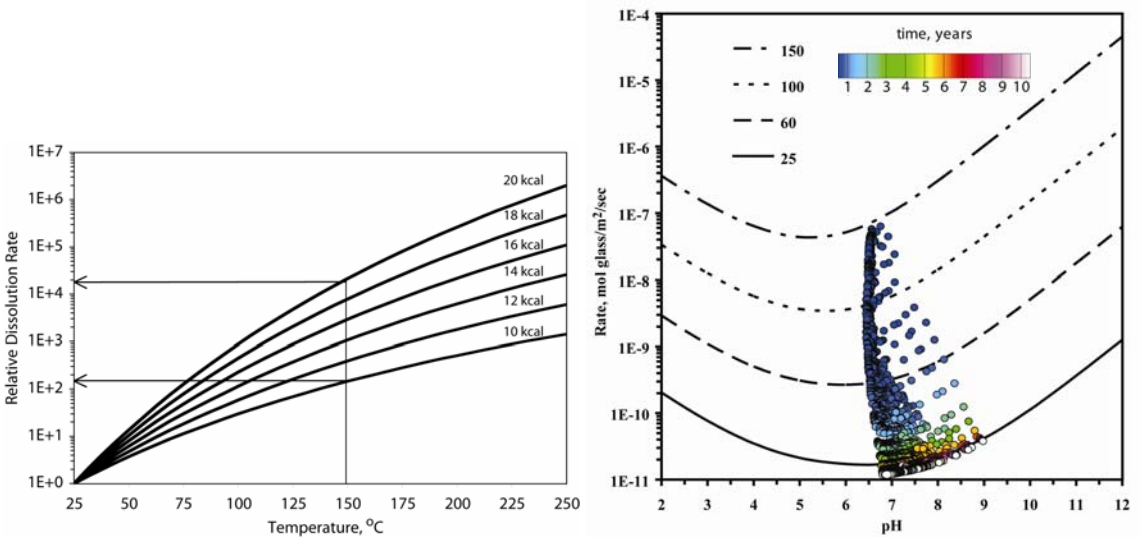


FIGURE 10. The effect of activation energy and temperature on dissolution rates as a function of temperature (left) and glass dissolution rates from streamline simulations superimposed on model glass dissolution rates as a function of pH and temperature for activation energy of 15 kcal/mole and ignoring saturation effects (right).

The glass dissolution activation energy, $E_a$ typically ranges from 10 to 20 kcal $mol^{-1}$ and has a dramatic effect on glass dissolution rates (Figure 10, left). For example, between 25 and 150ºC, glass dissolution rates may increase by factors of $10^2$ to $10^4$. However, $H^+$ and $OH^{-1}$, which are the principal dissolution-promoting aqueous species, will also be affected by temperature and, in turn, affect glass dissolution rates. A model of glass dissolution rates as a function of temperature and pH, based on the glass dissolution rate measurements of Mazer [1987] is shown in Figure 10 (right). The evolution of pH and glass dissolution rates in our reactive transport simulations is shown in Figure 10 as well.

Fluid velocity, which is affected by temperature (Figure 8, left), can affect the saturation term, [*1–Q/K(T)*], in equation (1). In our model, the *K(T)* term is defined by the solubility product of amorphous silica while Q is defined as the activity of $SiO_2$(aq). The activity of $SiO_2$(aq) will be affected by rate of glass dissolution (which releases $SiO_2$(aq)), rate of secondary silicate mineral precipitation (which sequesters $SiO_2$(aq)), and fluid velocity in the glass zone (which affects build-up of $SiO_2$(aq) in the glass zone).

Figure 11 compares streamline simulation of glass dissolution rate to temperature, pH, and $SiO_2$(aq) concentration at 0.0266, 0.72, and 9.0 years after the Cambric test. Between 0.0266 and 9.0 years, simulated melt glass dissolution rates decrease from about $5\times10^{-8}$ to $1\times10^{-11}$ moles/$m^2$/s, affected primarily by temperature. While the melt glass is relatively hot, the pH remains near 6.5 in the melt glass zone (compared to 8.5 under ambient conditions). With time, the pH tends to increase to a range of 7 to 9. The evolution of pH is primarily affected by temperature and the precipitation of clay secondary phases. The evolution of $SiO_2$(aq) concentrations in the glass zone is primarily driven by changes in the solubility of cristobalite ($\alpha/\beta$-$SiO_2$) secondary phases which are temperature-dependent. Fluid velocity and pH play a secondary role on $SiO_2$(aq) concentration.

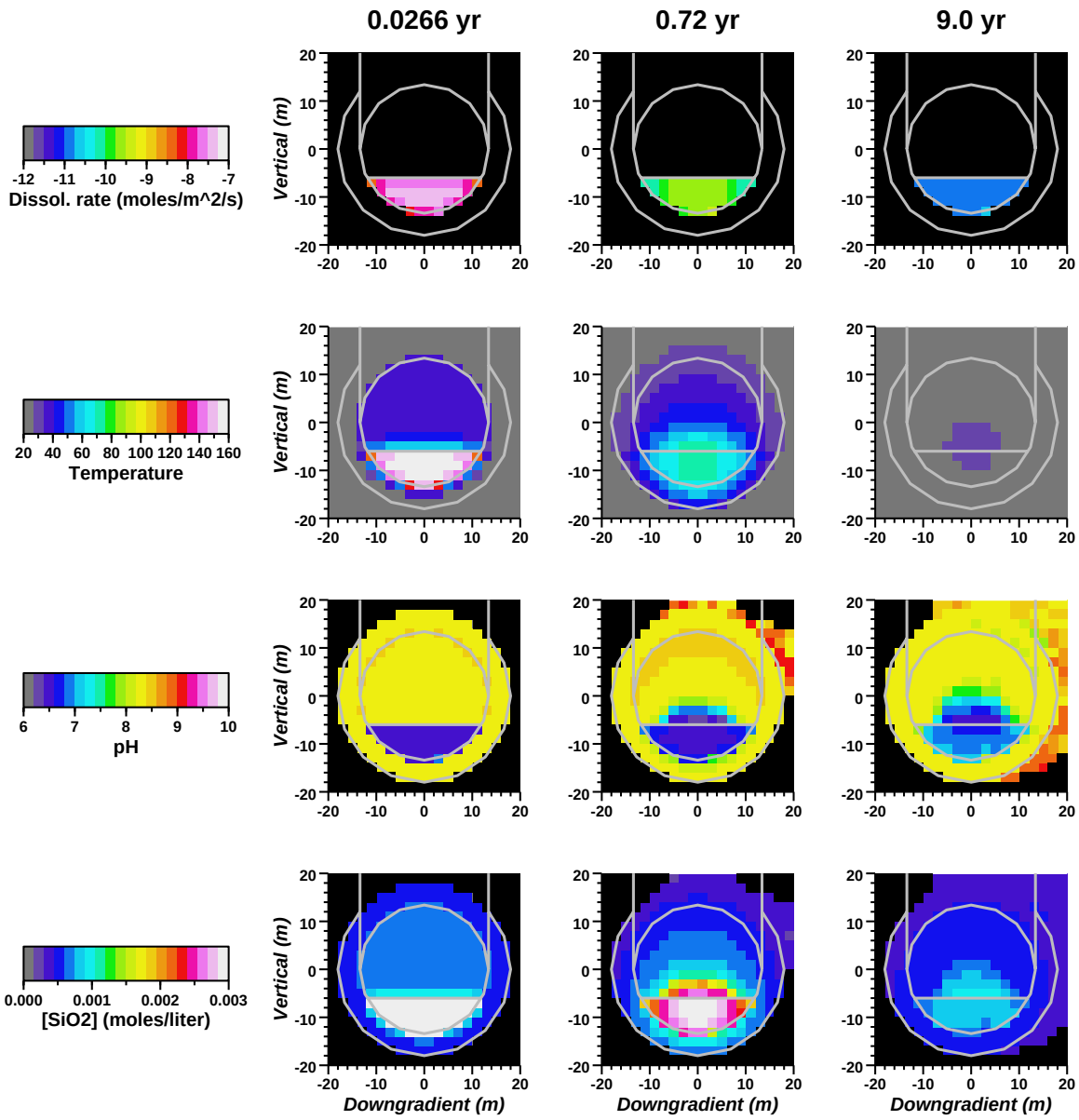


FIGURE 11. Streamline simulation of melt glass dissolution rate, temperature, pH, and $SiO_2$ concentration at 0.0266, 0.72, and 9.0 years since Cambric test. Areas shaded in black indicate zones where reactive transport was not simulated.

3.3. **Simulated Radionuclide Migration at Cambric.** The radionuclide "inventory" prescribes the quantities of radionuclides released by the nuclear test. The unclassified radionuclide inventory associated with the Cambric test includes 41 radionuclides, including different isotopes of the same element, 5 of which have very small inventories or are predominantly of natural origin (e.g. $^{40}K$). Thus, the transport of 36 radionuclides was evaluated in our simulations. Our reactive transport simulations distinguished 11 sorbing and 2 non-sorbing radionuclide classes which combined multiple isotopes of the same element and/or radionuclides expected to have similar reactive transport properties. From the 13 radionuclide classes, the transport behavior of all 36 radionuclides could be de-convolved.

Sorption of radionuclides to minerals and aqueous speciation was based on surface complexation, ion exchange, and aqueous speciation thermodynamic parameters and mineral characteristics reported elsewhere [Zavarin and Bruton, 2004a,b; Zavarin et al., 2002; Tompson et al., 2005]. Minerals addressed in the surface complexation/ion exchange model included iron oxide, smectite, clinoptilolite, illite/mica, and calcite. Sorbing radionuclide classes included $^{41}$Ca, $^{59,63}$Ni, $^{90}$Sr, $^{135,137}$Cs, $^{151}$Sm, $^{150,152,154}$Eu, $^{232,233,\ 234,235,236,238}$U, $^{237}$Np, $^{238,239,240,242}$Pu, $^{241}$Pu, and $^{241}$Am. $^{241}$Pu was distinguished from other Pu isotopes because it decays to $^{241}$Am, which is also a radionuclide of interest.

Dissolution of melt glass will contribute most significantly to concentrations of the more refractory radionuclide species and their daughter products. To assess the contribution of melt glass dissolution over time, the streamline-based reactive transport simulations tracked fluid containing dissolved melt glass by including one mole of non-sorbing tracer in the melt glass. The first column of images in Figure 12 shows simulated concentration fields for a tracer released from dissolving melt glass. The evolution of the melt glass zone tracer concentration field before 10 years shows two main impacts of test-related heat: (1) rapid increase in concentrations in the melt glass zone before 1 year, and (2) upward advection from the melt glass zone caused by thermally-induced groundwater flow in the upward direction. By 25.6 years, tracer concentrations in the melt glass zone drop about two orders-of-magnitude as a result of decreased melt glass dissolution rates and pumping from RNM-2S.

The second and third columns of images in Figure 12 show simulated concentration fields for the radionuclides $^{237}$Np and $^{241}$Pu. The initial $^{237}$Np and $^{241}$Pu *aqueous* concentrations are uniform in a spherical source zone including the melt glass zone, cavity, compressed zone, and lower chimney. However, the majority (95%) of the $^{237}$Np and $^{241}$Pu is incorporated initially in the melt glass. $^{237}$Np is very mobile while $^{241}$Pu is relatively immobile. Increases of $^{237}$Np and $^{241}$Pu concentration in the melt glass zone evident before 10 years are attributed to melt glass dissolution. Thermal effects before 1.0 year dominate change in concentration of $^{237}$Np in the melt glass zone before 10 years. Temporal change in $^{241}$Pu concentration is visibly affected the $^{241}$Pu half-life of 14.4 years. The pumping-induced transport of $^{237}$Np and $^{241}$Pu evident at 25.6 years highlights differences in radionuclide mobility. The $^{237}$Np plume reaching well RNM-2S is derived from a combination of $^{237}$Np distributed initially in the aqueous phase and resulting from glass dissolution. The $^{241}$Pu plume, however, is highly retarded and shows only a few meters of motion toward RNM-2S along flow paths originating from the melt glass zone.

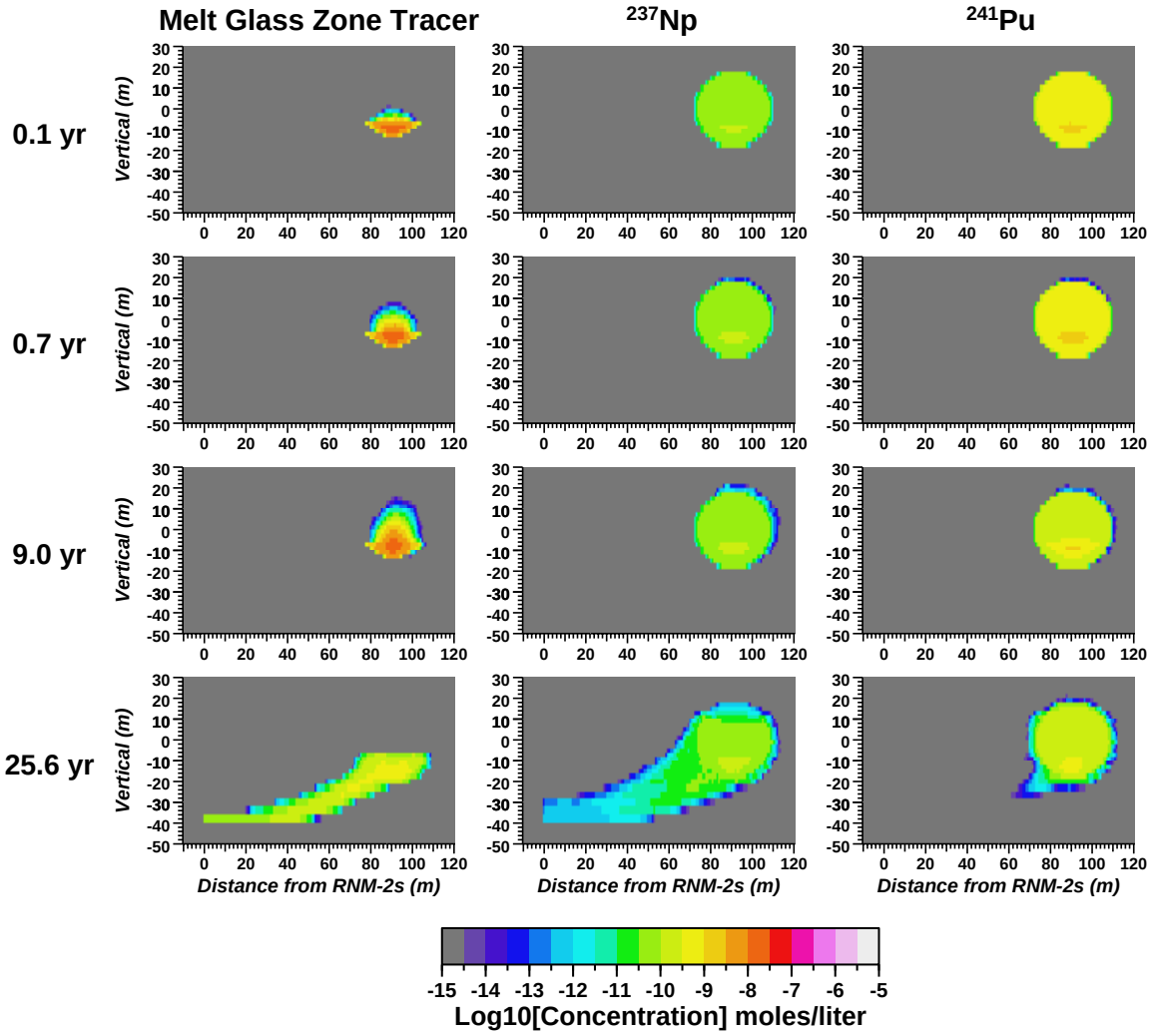


FIGURE 12. Oblique cross-sections through pumping well RNM-2S and center of Cambric test-altered zones showing simulated concentration fields for melt glass zone tracer, $^{237}$Np, and $^{241}$Pu at 0.1, 0.7, 9.0, and 25.6 years after the Cambric test.

## 4. SUMMARY AND CONCLUSIONS

In simulation of radionuclide migration resulting from an underground nuclear test, temperature affects reactive transport primarily by changing the flow velocity field and increasing rates of melt glass dissolution rates and secondary mineral precipitation. Thermal effects on groundwater flow can increase flow velocities by orders of magnitude over ambient conditions, cause convection cells and recirculation, and induce a significant upward flow velocity component relative to the ambient flow field. Rates of melt glass dissolution can increase by orders of magnitude.

The use of a streamline simulation method enables three-dimensional coupling of transient non-isothermal and variably saturated flow and nonlinear reactive geochemistry processes. The

streamline framework ensures feedback between transient flow velocity, temperature, and reactive transport processes. This capability is particularly important for typical underground nuclear test scenarios involving test-related heat, which induces thermal conditions near boiling temperature in the melt glass zone. If thermal effects are not accounted for, the fraction of radionuclides released into solution from melt glass dissolution could be vastly underestimated, particularly at early time.

The non-isothermal flow and radionuclide transport simulation results presented in this paper are consistent with a diverse collection of field experimental and characterization data acquired subsequent to the Cambric test. Observations from the Cambric radionuclide migration experiment in alluvium at the Nevada Test Site, Nevada, showed that only non-sorbing and weakly sorbing radionuclide species were significantly mobilized to scales of tens of meters or more following over 15 years of vigorous pumping-induced groundwater flow velocities. Our multi-component simulations of radionuclide transport behavior resulting from the Cambric underground nuclear test consider the combined effects of transient groundwater and heat flow. The simulations indicate transport of non-sorbing and weakly sorbing species can be influenced by transient thermal convection cells, while more sorbing species remain nearly immobile regardless of thermal and stressed groundwater flow conditions.

## ACKNOWLEDGMENTS

This work was performed under the auspices of the U.S. Department of Energy by Lawrence Livermore National Laboratory under contract No. W-7405-Eng-48.

## REFERENCES

Borg, I., R. Stone, H. B. Levy, and L. D. Ramspott , 1976, Information Pertinent to the Migration of Radionuclides in Ground Water at the Nevada Test Site, Part 1: Review and Analysis of Existing Information. UCRL-52078, Lawrence Livermore National Laboratory, Livermore, CA.

Bryant, E. A., 1992, The Cambric Migration Experiment: A Summary Report. LA-12335-MS, Los Alamos National Laboratory, Los Alamos, NM.

Burkhard, N. R. and J. T. Rambo, 1991, One Plausible Explanation for Groundwater Mounding, in Proc. Of the 6th Containment of Underground Nuclear Explosions, CONF-9109114, Vol. 2, Lawrence Livermore National Laboratory, Livermore, CA.

Carle, S. F., Maxwell, R M, and Pawloski, G. A. 2003, Impact of Test Heat on Groundwater Flow at Pahute Mesa, Nevada Test Site. UCRL-ID-152599, Lawrence Livermore National Laboratory, Livermore, CA, 143 p.

Finnegan, D. L., and Thompson, J. L., 2002, Laboratory and Field Studies Related to Radionuclide Migration at the Nevada Test Site in Support of the Underground Test Area and Hydrologic Resources Management Projects. LA-13919-MS, Los Alamos National Laboratory, Los Alamos, NM.

Germain, L. S. and J. S. Kahn, 1968, Phenomenology and Containment of Underground Nuclear Explosions. UCRL-50482, Lawrence Livermore National Laboratory, Livermore, CA.

Halford, K. J., Laczniak, R. J., and Galloway, D. L., 2005, Hydraulic Characterization of Overpressured Tuffs in Central Yucca Flat, Nevada Test Site, Nye County, Nevada. Scientific Investigations Report 2005-5211, U.S. Geological Survey, 55 p.

Knox, J. B., D. E. Rawson, and J. A. Korve, 1965, Analysis of a Groundwater Anomaly Created by an Underground Nuclear Explosion. Journal of Geophysical Research, v. 70, n. 4, p. 823–835.

Hoffman, D. C., R. Stone, and W. W. Dudley, Jr., 1977, Radioactivity in the Underground Environment of the Cambric Nuclear Explosion at the Nevada Test Site, LA-6877-MS, Los Alamos National Laboratory, NM.

Maxwell, R. M., Tompson, A. F. B., Carle, S. F., Zavarin, M., and Kollet, S. J., 2006, A Serendipitous, Long-term Infiltration Experiment: Water and Radionuclide Circulation Beneath the Cambric Trench at the Nevada Test Site. for CMWR XVI, Lawrence Livermore National Laboratory, Livermore, CA.

Mazer, J.J.,1987, Kinetics of Glass Dissolution as a Function of Temperature, Glass Composition, and Solution pHs. Ph.D. thesis, Northwestern University.

Nitao, J. J., 1999, User's Manual for the USNT Module of the NUFT Code, Version 2.0. UCRL-MA-130651, Lawrence Livermore National Laboratory, Livermore, CA.

Office of Technology Assessment, 1989, The Containment of Underground Explosions. United States Congress, OTA-ISC-414, Office of Technology Assessment.

Pawloski, G.A., 1999, Development of Phenomenological Models of Underground Nuclear Tests on Pahute Mesa, Nevada Test Site—Benham and Tybo, UCRL-ID-136003, Lawrence Livermore National Laboratory, Livermore, CA.

Pawloski, G. A., Tompson A. F. B., and Carle S. F., eds., 2001, Evaluation of the Hydrologic Source Term for Underground Nuclear Tests on Pahute Mesa and the Nevada Test Site: The Cheshire Test. Contributors: W.L. Bourcier, C.J. Bruton, S.F. Carle, J.I. Daniels, R.M. Maxwell, G.A. Pawloski, D.S. Shumaker, D.K. Smith, A.F.B. Tompson, and M. Zavarin, UCRL-ID-147023, Lawrence Livermore National Laboratory, Livermore, CA.

Pollock, D. W. , 1988, Semi-Analytical Computation of Path Lines for Finite-Difference Models. Ground Water, v. 26, n 6, p. 743-750.

Ramspott, L. D., and McArthur, R. D., 1977, Results of the Exploratory Drill Hole Ue5n, Frenchman Flat, Nevada Test Site. UCID-17392, Lawrence Livermore Laboratory, Livermore, CA, 35 p.

Steefel, C. I. and S. B. Yabusaki, 1996, OS3D/GIMRT, Software for Modeling Multicomponent and Multidimensional Reactive Transport, User Manual and Programmer's Guide, Version 1.0. PNL-11166, Pacific Northwest National Laboratory, Richland, WA.

Tompson, A.F.B., Maxwell, R.M., Carle, S.F., Zavarin, M., Pawloski, G.A., Shumaker, D.E, 2005, Evaluation of the Non-Transient Hydrologic Source Term from the CAMBRIC Underground Nuclear Test in Frenchman Flat, Nevada Test Site. UCRL-TR-217191, Lawrence Livermore National Laboratory, Livermore, CA, 62p.

Tompson, A. F. B., Hudson, G. B., Smith, D.K., and Hunt, J. R., 2006, Analysis of Radionuclide Migration through a 200-m Vadose Zone Following a 16-year Infiltration Event. Advances in Water Resources, v. 29, p. 281-292.

U.S. Department of Energy, 2000, United States Nuclear Tests July 1945 through September 1992. DOE/NV—209-REV 15, Nevada Operations Office, 180 p.

Warren, R. G., Benedict F. C., Jr., Rose T. P., Smith D. K., Chipera S. J., Kluk E. C., and Raven K. M.., 2002, Alluvial Layering and Distribution of Reactive Phases within Drill Holes ERt/4 and UE5n of Frenchman Flat. LA-UR-02-6206, Los Alamos National Laboratory, Los Alamos, NM.

Zavarin M. and Bruton C. J., 2004a, A Non-Electrostatic Surface Complexation Approach to Modeling Radionuclide Migration at the Nevada Test Site, Aluminosilicates. UCRL-TR-208672, Lawrence Livermore National Laboratory, Livermore, CA.

Zavarin M. and Bruton C. J., 2004b, A Non-Electrostatic Surface Complexation Approach to Modeling Radionuclide Migration at the Nevada Test Site, Iron Oxides and Calcite. UCRL-TR-208673, Lawrence Livermore National Laboratory, Livermore, CA.

Zavarin M., Roberts S. K., Rose T. P., and Phinney D. L., 2002, Validating Mechanistic Sorption Model Parameters and Processes for Reactive Transport in Alluvium. UCRL-ID-149728, Lawrence Livermore National Laboratory, Livermore, CA.